

Structural and Functional Connectivity of Visual Cortex in Schizophrenia and Bipolar Disorder: A Graph-Theoretic Analysis

Eric A. Reavis^{*1,2,⊙}, Junghee Lee^{1,2}, Lori L. Altshuler^{†,1}, Mark S. Cohen^{3,4}, Stephen A. Engel⁵, David C. Glahn⁶, Amy M. Jimenez^{1,2,⊙}, Katherine L. Narr¹, Keith H. Nuechterlein^{1,3}, Philipp Riedel^{1,7}, Jonathan K. Wynn^{1,2}, and Michael F. Green^{1,2}

¹Semel Institute for Neuroscience and Human Behavior, University of California, Los Angeles, Los Angeles, CA 90024; ²Desert Pacific Mental Illness Research, Education, and Clinical Center Greater Los Angeles VA Healthcare System, Los Angeles, CA 90073; ³Department of Psychology, University of California, Los Angeles, Los Angeles, CA 90024; ⁴Departments of Neurology, Radiology, Biomedical Physics, and Bioengineering University of California, Los Angeles, Los Angeles, CA 90024; ⁵Department of Psychology, University of Minnesota, Minneapolis, MN 55455; ⁶Tommy Fuss Center for Neuropsychiatric Disease Research, Department of Psychiatry Boston Children's Hospital and Harvard Medical School, Boston, MA 02115; ⁷Department of Psychiatry and Psychotherapy, University Hospital Carl Gustav Carus, Medical Faculty, Technische Universität Dresden, Dresden, Germany

[†]Deceased.

*To whom correspondence should be addressed; 760 Westwood Plaza, Room 27-440, Los Angeles, CA 90024, US; tel: 310-794-5586, fax: 310-268-4056, e-mail: ereavis@ucla.edu

Visual processing abnormalities in schizophrenia (SZ) are poorly understood, yet predict functional outcomes in the disorder. Bipolar disorder (BD) may involve similar visual processing deficits. Converging evidence suggests that visual processing may be relatively normal at early stages of visual processing such as early visual cortex (EVC), but that processing abnormalities may become more pronounced by mid-level visual areas such as lateral occipital cortex (LO). However, little is known about the connectivity of the visual system in SZ and BD. If the flow of information to, from, or within the visual system is disrupted by reduced connectivity, this could help to explain perceptual deficits. In the present study, we performed a targeted analysis of the structural and functional connectivity of the visual system using graph-theoretic metrics in a sample of 48 SZ, 46 BD, and 47 control participants. Specifically, we calculated parallel measures of local efficiency for EVC and LO from both diffusion weighted imaging data (structural) and resting-state (functional) imaging data. We found no structural connectivity differences between the groups. However, there was a significant group difference in functional connectivity and a significant group-by-region interaction driven by reduced LO connectivity in SZ relative to HC, whereas BD was approximately intermediate to the other 2 groups. We replicated this pattern of results using a different brain atlas. These findings support and

extend theoretical models of perceptual dysfunction in SZ, providing a framework for further investigation of visual deficits linked to functional outcomes in SZ and related disorders.

Key words: schizophrenia/bipolar disorder/visual processing/structural connectivity/functional connectivity, graph theory

Introduction

Schizophrenia (SZ) is characterized by specific cognitive deficits associated with poor functional outcomes.¹ Such deficits have been identified across multiple cognitive domains, including perception, attention, memory, executive functioning, social cognition, and others.² Bipolar Disorder (BD) shares genetic risk factors and phenotypic characteristics with SZ.³⁻⁸ Extensive work has identified cognitive deficits in overlapping domains (eg, attention, memory, executive functioning) among persons with BD.³⁻⁵ In general, current evidence suggests that SZ and BD are associated with similar types of cognitive impairments, though deficits tend to be milder in BD.^{4,5}

In SZ, many studies have identified specific, persistent deficits in the cognitive domain of visual perception using performance-based tests to assess backward masking,

contour integration, motion discrimination, and illusion perception, among other perceptual phenomena.^{6–10} Importantly, performance on such visual tests predicts everyday functioning in SZ, suggesting that visual perception deficits might have important cascading effects on other types of processing.⁷ Whereas early work in BD seldom assessed perception, emerging evidence suggests that there may be overlapping perceptual processing deficits for SZ and BD.^{11,12} Considering the overlap of various cognitive deficits between SZ and BD, it is possible that perceptual deficits could relate to impaired functioning in BD also. Therefore, improved understanding of factors that contribute to perceptual deficits in SZ and BD could help identify treatment targets for improvement of everyday functioning in both disorders.

The neural factors that result in visual perceptual dysfunction in SZ and BD remain poorly understood, but abnormalities in visual cortex appear to contribute. In particular, an object-selective region of lateral occipital cortex (LO) has been associated with various perceptual deficits. LO has been shown to function abnormally during masking and contour integration tasks in SZ,^{13,14} and during an object discrimination task in both SZ and BD.¹⁵ By contrast, early visual cortex (EVC) function has been found to be relatively normal during such tasks, though some studies have found subtle deficits linked to EVC.^{13,16,17} Related theoretical models of perceptual dysfunction in SZ have posited that early-stage visual processing (eg, in EVC) is relatively normal, but processing abnormalities emerge and compound as information progresses through more advanced stages of processing.¹⁸

Despite considerable evidence of abnormal functioning for specific nodes within the visual processing network during visual processing tasks in SZ and BD, little is known about the connectivity of the visual system in these disorders. If the flow of information to, from, or within the visual system is disrupted by reduced connectivity, this could help to explain perceptual deficits.

MRI can be used to examine both structural and functional connectivity. Structural connectivity is typically assessed using diffusion-weighted imaging (DWI), which provides a basis for measuring the organization and strength of white matter connections between brain areas. Functional connectivity refers to patterns of correlated activity across brain areas; it can be measured using functional MRI (fMRI) and is often assessed during a task-free resting-state scan.

Many studies have evaluated structural and functional connectivity in SZ and BD, but rarely in the same study. Most connectivity studies have performed whole-brain analyses rather than hypothesis-driven investigations of specific regional networks, and findings have been mixed. Multiple studies have reported structural or functional dysconnectivity in people with SZ or BD.^{16–22} In general, whole-brain connectivity findings vary considerably across studies, and contradictory results exist in the literature.^{19–21}

The many whole-brain studies of structural and functional connectivity do not address whether specific nodes of the visual processing network are connected abnormally in SZ or BD. To our knowledge, no study has performed hypothesis-driven comparisons of connectivity among different visual system nodes in these disorders. Thus, although there has been considerable research on structural and functional connectivity in SZ and BD, it is not clear from the existing literature whether the connectivity of visual areas that have been identified specifically as dysfunctional during task-based fMRI (eg, LO) is normal or abnormal.

The present study aimed to address this question with a targeted investigation of EVC and LO connectivity. We used a parallel approach to estimate both structural and functional connectivity in these areas, defining network nodes according to the same anatomical parcellation for both modalities, and using the same graph-theoretic measures of connectivity for both modalities. The main goal of the study was to examine the connectivity of specific visual system nodes. We selected local efficiency as our primary measure as it is among the most common indices of nodal connectivity.^{22–27} In keeping with earlier studies, we also computed a brain-wide measure of connectivity—global efficiency—for each modality. Local efficiency captures the fault tolerance of a topological neighborhood of nodes (ie, the capacity for information transfer between adjacent nodes when a node of interest is removed).²⁸ Global efficiency indexes the parallel processing efficiency of the entire network.²⁸

Based on findings from task-based fMRI and *a priori* predictions based on theory, we hypothesized that SZ and BD would show reductions in both structural and functional local efficiency, and that those reductions would be greater in a mid-level visual area (LO) than in EVC. While we had strong theoretical reasons to focus *a priori* on group-by-region interactions involving EVC and LO, we were also interested to know whether local efficiency might differ by group for other regions of visual cortex. Therefore, we performed exploratory comparisons of local efficiency across groups for other nodes included in the anatomical parcellation of the occipital lobe (cuneus and lingual gyrus). We also performed a confirmatory analysis of significant findings using a different brain atlas.

Methods and Materials

Participants

Participants in this study came from an NIMH-sponsored investigation of visual processing in major mental illness. Some of the data from the project have been included in previous publications that tested distinct hypotheses, including an investigation of relationships between resting-state connectivity and social processing,²⁹ and a targeted

investigation of the structural connectivity of the optic radiations.³⁰

Detailed recruitment information and selection criteria for all participants are provided in the [supplementary methods](#) and briefly summarized here. All patient participants were clinically stable outpatients with a DSM-IV diagnosis of SZ or BD based on a structured clinical interview (SCID).³¹ Members of those 2 groups were on clinically-determined doses of medication and tested outside of mood episodes.

In total, 149 participants completed both a DWI scan and a resting-state fMRI scan. However, 6 participants were excluded for reasons related to resting-state motion ([supplementary methods](#)). In addition, 1 participant was excluded due to poor brain coverage during fMRI, and 1 participant was excluded because of technical problems. Thus, the usable sample for all analyses described in this paper was 141 participants, including 48 SZ, 46 BD, and 47 HC.

MRI Data Collection

All MRI data were collected at the UCLA Staglin Center for Cognitive Neuroscience on a 3-Tesla Siemens Tim Trio scanner with a 12-channel head coil (Siemens Medical Solutions; Erlangen, Germany). T1, DWI, and resting-state fMRI scans were collected using standard parameters described in detail in the [supplementary methods](#).

MRI Data Analysis

A brief summary of the methods used for MRI data analysis is included in this section. For a detailed description of all MRI processing steps, see the [supplementary methods](#). There were 3 overarching steps for the MRI data analysis: defining network nodes based on automated segmentation of structural scans using FreeSurfer,³² processing of resting-state fMRI data using FSL,^{33,34} and processing of DWI data using MRtrix3.³⁵

T1 Anatomical Data Analysis (Defining Nodes). Individualized anatomical nodes for both functional and structural connectomic analyses were created from each subject's high-resolution T1 scan using the Desikan-Killiany Atlas.³⁶ In order to focus on identical areas of interest across modalities, the same anatomical parcellation was used for both structural and functional connectivity analyses, rather than using a different atlas for each. The primary nodes of interest for the study corresponded to the pericalcarine (ie, EVC) and LO labels. We also performed post hoc exploratory analyses of 2 adjacent occipital labels: the lingual gyrus and cuneus.

In order to confirm that significant results of the primary analyses were not atlas-dependent, we performed a replication of significant findings using a different

parcellation scheme. For these analyses, we parcellated the brain into nodes according to the multimodal Glasser atlas as described in the [supplementary methods](#) and repeated the graph analyses using the same methods with this new set of nodes. The Glasser parcellation scheme was developed from multimodal Human Connectome Project MRI data to divide the cortical surface into 180 regions per hemisphere based on both structural and functional characteristics.³⁷

Resting-State fMRI Analysis. A multi-step approach was used to characterize and correct motion during the resting-state fMRI scans, including 3-stage affine motion correction using MCFLIRT³⁸ and removal of residual motion effects using ICA-AROMA.³⁹ A detailed description of the approach to motion correction and other preprocessing (eg, skull stripping, spatial smoothing, high-pass temporal filtering) is provided in the [supplementary methods](#). Mean resting-state timecourses for each FreeSurfer node were extracted from the motion-corrected and preprocessed data using `fslmeans`. Cross-correlations for the timecourses of each pair of regions were computed to produce a complete connectomic matrix of functional connectivity. Negative values were made positive before graphs were created and analyzed. In some cases, rectifying negative correlations in this way can yield different results than excluding negative values from graph analyses. We performed follow-up analyses of the resting state connectomes that excluded negative correlations to rule out this possibility.

DWI Data Analysis. Quality checks of the DWI data were performed using FSL ([supplementary methods](#)). Following the quality control steps, preprocessing of raw DWI data for tractography was performed using MRtrix3, as described in the [supplementary methods](#).³⁵ After the DWI data were preprocessed, anatomically constrained probabilistic tractography was performed in MRtrix3 to produce a connectome matrix of the estimated strength of white-matter connections (ie, the apparent fiber density, based on the SIFT2 algorithm^{40,41}) between each pair of FreeSurfer-defined cortical and subcortical nodes for each participant, analogous to the functional connectome matrix.⁴² [Figure 1](#) shows an example tractogram. Details of the approach to probabilistic tractography are included in the [supplementary methods](#).

Graph Analyses and Statistics

We used the Brain Connectivity Toolbox²³ in MATLAB to calculate separate graph-based global and local efficiency scores for the structural and functional connectome matrices. Efficiency scores were calculated from thresholded (ie, binarized) connectome matrices, in which connections above a specific threshold are considered present and connections below that threshold

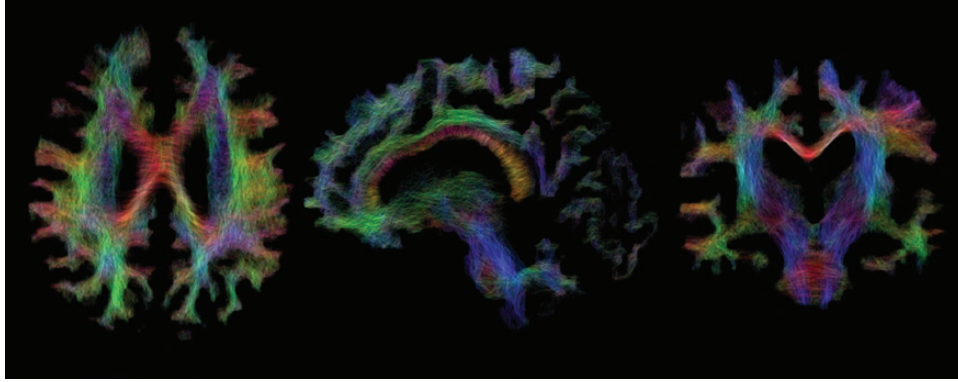


Fig. 1. Example DWI tractogram from one SZ participant in native anatomical space (axial, sagittal, and coronal views, downsampled to 200k streamlines for display purposes). Each line represents one streamline. Line colors are assigned according to the primary directional axis of the streamline.

are considered absent. We had no *a priori* interest in a particular threshold and wanted to avoid biasing the results according to the range of thresholds selected, so we used the common technique of parametrically varying thresholds across a broad range and calculating the area under the resulting curve (AUC), a technique that has been employed in other studies focused on graph-based measures.⁴³ AUC values calculated in this way thus reflect threshold-independent measures of efficiency. For the structural connectivity matrices, the data were thresholded by the number of streamlines connecting each pair of nodes (range: 100–100 000). For the functional connectivity matrices, correlation thresholds were applied (range: $r = .1$ – 1.0). At each threshold, efficiency scores were averaged across brain hemispheres, since visual cortex ROIs are highly symmetrical. AUCs for bilateral global and local efficiency over these ranges were used as the dependent variables in all statistical tests.

This procedure, using absolute thresholds to define graphs, is the preferred method for brain graph analysis when nodal statistics are of primary interest, but it can lead to confounding group differences in the number of edges present in the resulting graphs (ie, differences in network density) in some datasets.^{44,45} Therefore, the current recommended best practice is to first test for group differences in network density and then include network density as a covariate in subsequent analyses if any such differences are found.^{44,45} This was the approach we took in the present study.

Because a direct comparison of structural vs functional connectivity would not be interpretable (ie, connectivity estimates will naturally be higher in one modality than the other), separate, parallel statistical analyses were conducted for each modality. In each, one ANOVA was performed to test the hypothesis that global efficiency would differ across groups. A second ANOVA in each modality was performed to test the hypothesis that patient-control differences in local efficiency would be more

pronounced in LO than EVC (ie, a group by region interaction). Follow-up tests were used to clarify the interpretation of significant effects in the ANOVAs. Replication of significant findings was performed using the Glasser atlas to confirm that results were not atlas-dependent.

To assess whether structural and functional connectivity were related within or between EVC and LO, we also correlated local efficiency scores between the 2 regions and the 2 modalities within each group. Due to the relatively large number of tests, Bonferroni correction was applied to the significance threshold for these analyses. Possible group differences in correlation magnitudes were assessed using Fisher's Z transformation.

In order to identify possible relationships between medication dosage and connectivity, we calculated chlorpromazine-equivalent antipsychotic dosages and looked for correlations with the connectivity measures. Specifically, we calculated equivalent dosages for members of the SZ and BD groups who had sufficient medication information available, using published conversion factors.^{46,47} As for the other correlations, we performed Bonferroni correction for these analyses to avoid false-positive results due to the number of tests.

Results

Participants

Table 1 contains demographic and clinical information about the included participants. Age, handedness, and parental education did not differ significantly across the 3 groups. As expected, the SZ group had fewer years of personal education. The 2 patient groups were well-matched for illness duration and did not differ on the HAM-D or YMRS scales. The SZ group had significantly higher BPRS scores than the BD group.

Members of the BD group were tested outside of mood episode. Within the BD group, 12 participants had a history of psychosis and 34 did not. Twenty-nine had a diagnosis of BD I and 17 had a diagnosis of BD

II. To investigate possible differences in structural and functional connectivity between these BD subgroups, we performed exploratory follow-up ANOVAs that focused on those BD groups. None showed any significant effects of diagnosis or psychosis history ([supplementary table 3](#)).

While there was no significant difference in participant sex across groups, there was a trend toward a group difference ($P = .07$). Some previous studies in healthy samples have found sex differences in graph-theoretic measures of connectivity, including global and local efficiency, particularly for tractography-based measures of structural connectivity.^{48,49} In fact, consistent with these findings, we found higher global structural connectivity in females than males in our data ($F(1,134) = 12.27, P < .01, \eta_p^2 = 0.08$) but no group by sex interaction ($F(2,134) = 0.47, P = .63, \eta_p^2 = 0.01$). We did not find any sex effects on local efficiency measures of structural connectivity or on any functional connectivity measures. Considering the sex effect on global efficiency in our structural data, we included sex as a factor of non-interest in all ANOVAs.

Structural Connectivity

There was no significant difference in network density across groups ($F(2,134) = 0.73, P = .48, \eta_p^2 = 0.01$), so no statistical correction for network density was required in subsequent tests.^{44,45} We found no significant group difference in global efficiency ($F(2,134) = 2.11, P = .13, \eta_p^2 = 0.03$). [Supplementary figure 1](#) shows global efficiency scores over the full range of thresholds by group and sex.

We compared local efficiency scores between EVC and LO in a repeated-measures ANOVA with a fixed between-subjects factor *group*. This ANOVA identified a significant main effect of region ($F(1,134) = 953.01, P < .001, \eta_p^2 = 0.88$), with EVC showing higher local efficiency than LO. No other main effects or interactions were significant (group main effect: $F(2,134) = 0.44, P = .65, \eta_p^2 = 0.01$; group-by-region interaction: $F(2,134) = 0.61, P = .55, \eta_p^2 = 0.01$). Plots of local efficiency by region and group across the full range of streamline thresholds appear in [figure 2](#).

Table 1. Characterization of Participants Included in the Analyses

	SZ ($N = 48$)	BD ($N = 46$)	HC ($N = 47$)	Group Comparison	
	Mean (SD)	Mean (SD)	Mean (SD)	Statistic	P
Age	46.09 (11.59) Min = 21 Max = 63	43.98 (12.55) Min = 21 Max = 64	47.21 (8.18) Min = 30 Max = 63	$F(2,137) = 1.05$.35
Illness duration (y)	23.60 (12.76)	22.58 (12.75)		$t(85) = 0.37$.71
Personal education	12.87 (2.10)	14.13 (2.31)	14.36 (1.79)	$F(2,136) = 7.00$.001
Parental education	12.99 (2.89)	14.02 (2.64)	13.76 (2.68)	$F(2,128) = 1.67$.19
Sex (M/F)	31 / 16	23 / 23	20 / 27	$\chi^2(2) = 5.39$.07
Handedness (R/L)	41 / 6	41 / 4	40 / 7	$\chi^2(2) = 0.79$.67
BPRS (Total)	39.51 (10.38)	33.34 (5.35)		$t(89) = 3.53$.001
HAM-D (21-item Total)	7.17 (6.07)	7.08 (5.35)		$t(92) = 0.07$.95
YMRS (Total)	4.58 (4.05)	3.44 (4.46)		$t(91) = 1.29$.20

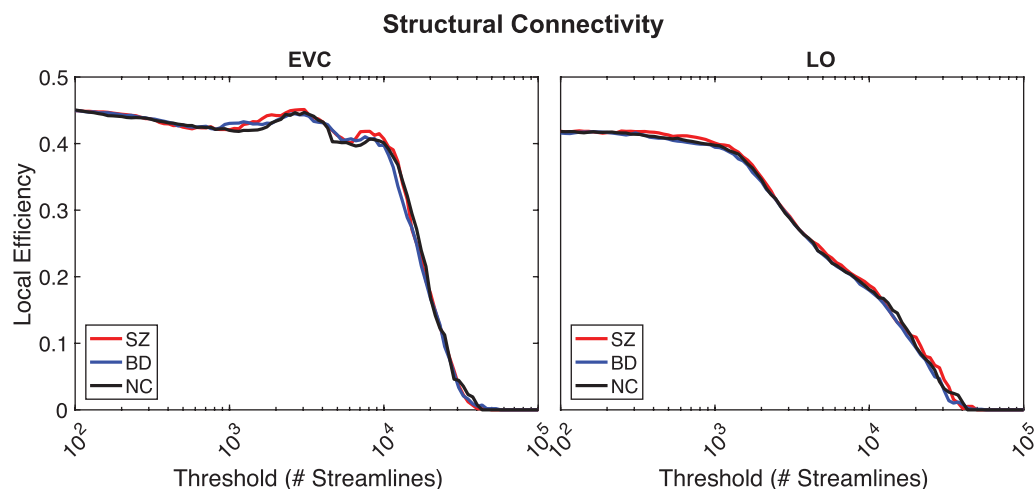


Fig. 2. Structural connectivity local efficiency scores for the 2 primary regions of interest (Early Visual Cortex & Lateral Occipital Cortex) across all thresholds.

Supplementary figure 2 shows the local efficiency scores by region, group, and sex. Exploratory analyses of local efficiency scores for the cuneus and lingual gyrus nodes showed no group differences (cuneus $F(2,134) = 0.81, P = .45, \eta_p^2 = 0.01$; lingual gyrus $F(2,134) = 0.09, P = .91, \eta_p^2 = 0.001$).

Functional Connectivity

Estimates of participant motion did not differ across groups (**supplementary tables 1 and 2**). Likewise, there was no significant difference in network density across groups ($F(2,134) = 1.29, P = .28, \eta_p^2 = 0.02$), so no statistical correction for network density was required in subsequent tests.^{44,45} We found no significant group difference in global efficiency scores ($F(2,134) = 1.09, P = .34, \eta_p^2 = 0.02$). The same pattern of results were obtained for network density and global efficiency when negative values were excluded. **Supplementary figure 3** shows the global efficiency scores across the full range of thresholds by group and sex.

As in the structural connectivity analysis, we compared functional-connectivity-based local efficiency scores between EVC and LO in a repeated-measures ANOVA with a fixed between-subjects factor *group*. This ANOVA identified a significant main effect of region ($F(1,134) = 32.82, P < .001, \eta_p^2 = 0.20$), with EVC showing higher local efficiency than LO. There was also a significant main effect of group ($F(2,134) = 3.63, P = .03, \eta_p^2 = 0.05$), and a significant group-by-region interaction ($F(2,134) = 3.27, P = .04, \eta_p^2 = 0.05$). The pattern of results was the same when negative values were excluded. Plots of local efficiency by region and group across the full range of functional connectivity thresholds appear in **figure 3**. **Supplementary figure 4** shows local efficiency by region, group, and sex.

Having identified a significant main effect of group and a group-by-region interaction, we performed post hoc analyses. Pairwise comparisons suggest that the group main effect was driven by differences between SZ and HC ($P = .008$); there were no significant differences between BD and HC or between BD and SZ ($P = .11$ and $P = .28$, respectively). To explore the group-by-region interaction, we conducted follow-up ANOVAs within EVC and LO. EVC showed no significant group difference ($F(2,134) = 1.03, P = .36, \eta_p^2 = 0.02$), but LO did show a group difference ($F(2,134) = 5.90, P = .004, \eta_p^2 = 0.08$). Further pairwise group comparisons for LO show greater local efficiency in HC than SZ ($P = .001$), and marginally greater local efficiency in HC than BD ($P = .053$), but no significant difference between BD and SZ ($P = .15$).

To further investigate the regional specificity of group differences in functional connectivity, we performed exploratory analyses of local efficiency for the cuneus and lingual gyrus (the 2 adjacent occipital regions included in the parcellation). The lingual gyrus showed a significant group difference in local efficiency, similar to LO ($F(2,134) = 5.78, P = .004, \eta_p^2 = 0.08$). Although the cuneus showed a trend in the same direction, local efficiency did not differ significantly across groups in the cuneus ($F(2,134) = 2.57, P = .08, \eta_p^2 = 0.04$).

In order to confirm that the significant results of the primary analyses were not atlas-dependent, we repeated the functional connectivity graph analyses using the Glasser atlas. We found a highly similar pattern of effects using this parcellation scheme. Specifically, we found significant group differences in each of the 3 sub-regions of LO but no significant group differences in V1, V2, V3, or V4 (**table 2**).

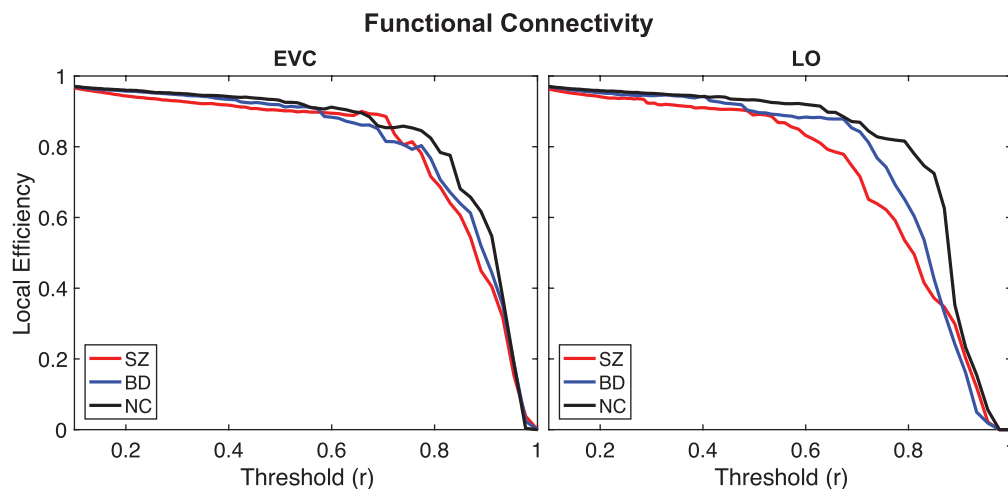


Fig. 3. Functional connectivity local efficiency scores for the 2 primary regions of interest (Early Visual Cortex & Lateral Occipital Cortex) across all thresholds.

Relationship Between Structural and Functional Connectivity

To assess potential relationships between structural and functional connectivity, as well as between EVC and LO, we calculated pairwise Pearson correlations for local efficiency across both regions and both modalities within each group. The pattern of results was the same across all 3 groups: consistent moderate correlations between the 2 regions within each modality but no significant correlations between modalities (table 3). Fisher’s *r*-to-*Z* tests showed no significant difference in the magnitude of any correlation between any pair of participant groups.

Relationship Between Medication Dosages and Connectivity

To evaluate possible relationships between medication dosage and connectivity, we calculated Pearson correlations between chlorpromazine-equivalent dosages and each primary connectivity metric. All correlations with local efficiency were clearly nonsignificant (*r* range: $-.10$ – $.10$). The correlation between antipsychotic medication and functional global efficiency was also nonsignificant ($r(62) = -.19$, $P = .14$). The correlation coefficient for chlorpromazine-equivalent dosage and structural global efficiency was somewhat higher ($r(62) = -.28$, $P = .03$), but this

Table 2. ANOVAs Comparing Functional Connectivity Across Groups for Visual ROIs in the Glasser Atlas (Replication Analysis)

Region	<i>F</i>	<i>P</i>	η_p^2	Significant Post Hoc Pairwise Comparisons
V1	0.94	.391	0.01	
V2	1.73	.182	0.03	
V3	2.10	.127	0.03	
V4	2.56	.081	0.04	
LO1	3.17	.045	0.05	HC > BD, <i>P</i> = .01; HC > SZ, <i>P</i> = .002
LO2	3.86	.023	0.06	HC > BD, <i>P</i> = .007; HC > SZ, <i>P</i> = .001
LO3	3.48	.034	0.05	HC > BD, <i>P</i> = .015; HC > SZ, <i>P</i> = .001

Note: Network density was included as a covariate in these ANOVAs due to a weak trend toward a group difference ($P = .12$).^{44,45} The results confirm significant effects found without the covariate. Results from the Desikan atlas (primary analysis) are presented separately in the main text. Regions indicated in bold type showed significant group differences at a level of $P < 0.05$.

Table 3. Local Efficiency Correlations Across Modalities and Regions, by Group

		Functional		Structural	
		EVC	LO	EVC	LO
Schizophrenia					
Functional	EVC	-	$r = .75, P < .001$	$r = -.22, P = .14$	$r = .11, P = .48$
	LO		-	$r = .004, P = .98$	$r = .03, P = .85$
Structural	EVC			-	$r = .52, P < .001$
	LO				-
Bipolar Disorder					
Functional	EVC	-	$r = .68, P < .001$	$r = .06, P = .68$	$r = .03, P = .84$
	LO		-	$r = .16, P = .29$	$r = .16, P = .29$
Structural	EVC			-	$r = .68, P < .001$
	LO				-
Healthy Controls					
Functional	EVC	-	$r = .56, P < .001$	$r = .06, P = .69$	$r = -.06, P = .69$
	LO		-	$r = .05, P = .74$	$r = .02, P = .90$
Structural	EVC			-	$r = .56, P < .001$
	LO				-

Note: EVC, early visual cortex; LO, lateral occipital cortex. Correlations indicated in bold type showed were statistically significant at a level of $P < 0.001$.

effect did not survive correction for the number of correlations performed.

Discussion

The goal of this study was to identify abnormalities in the structural and functional connectivity of visual cortex in SZ and BD. We found no evidence of group differences in structural connectivity, but we did find group differences in functional connectivity that were consistent with our hypotheses.

Specifically, functional local efficiency across LO and EVC (2 occipital regions previously investigated in task-based neuroimaging studies^{9–12}) was reduced in SZ, with a significant group-by-region interaction indicating a larger difference in LO than EVC. Further exploration of functional local efficiency identified one adjacent occipital node (the lingual gyrus) that showed a similar pattern of functional dysconnectivity to LO in SZ, while another (the cuneus) did not show a significant pattern of functional dysconnectivity. BD connectivity metrics were intermediate to the other 2 groups. In a replication using a different atlas, we again found significant group differences in connectivity for LO, but not for V1, V2, V3, or V4. We found all these effects using a wide, bias-free range of thresholds, although local efficiency differences appeared largest for high thresholds ($r \sim .6$ – $.9$).

By contrast, functional global efficiency of the whole brain network did not differ across groups using the same wide range of thresholds. Because of the lack of significant group differences in global connectivity, the fact that local connectivity measures showed a group-by-region interaction, and the fact that including global connectivity as a covariate did not change this pattern of results, the observed differences in functional connectivity cannot be attributed to confounding effects of total connectivity. Possible confounding differences in network density across groups were also ruled out.

Based on patterns of visual processing deficits, as well as patterns of abnormal and spared brain activity during visual perception tasks, it has been theorized that visual processing in SZ is relatively intact in EVC but becomes progressively more abnormal due to compounding errors in processing as information moves up the visual hierarchy.¹⁸ According to this model of visual processing deficits, mid- to high-level areas such as LO should show more pronounced processing abnormalities than early areas (eg, EVC). The present results lend additional support to this theoretical model. Indeed, the present findings further advance the model by demonstrating that such mid-level visual areas—but not EVC—show functional dysconnectivity in SZ, even when the structural connectivity of those same areas does not appear abnormal. The results also show a consistent pattern of intermediate functional dysconnectivity for mid-level visual cortex in BD. This fits well with the idea that BD

could represent an intermediate phenotype between SZ and HC, with a corresponding pattern of intermediate differences in neural functioning. Thus, further research to investigate the utility of this model for understanding visual processing abnormalities in BD is warranted.

The results of the current study are broadly in keeping with findings from other recent studies that evaluated functional connectivity in the visual system in SZ but did not specifically investigate structural and functional connectivity of individual cortical areas at different levels of the visual processing hierarchy. One such study found reduced synchronization of activity across visual areas at rest in SZ (ie, differences in modularity of visual cortex).⁵⁰ Another found abnormal functional connectivity throughout the dorsal and ventral visual pathways.⁵¹ A third study found diminished functional connectivity within visual cortex in SZ, which was correlated with impairments on a perceptual closure task.⁵²

The lack of group differences in structural connectivity was somewhat unexpected. However, few previous structural connectivity studies have specifically focused on the visual system. Recently, we published a targeted probabilistic tractography study based on a subset of the participants in the current sample, in which we found no group differences in the optic radiations (the primary thalamic input to EVC),³⁰ although another study using different methods did find differences between SZ and HC for that tract.⁵³ This is not to say that group differences in the structure of the visual system are entirely absent. In another recent publication, we examined the cortical thickness of EVC and LO in a subset of the current participants, and we found small but significant group differences, with thinnest cortex in SZ, thickest in HC, and intermediate thickness in BD.⁵⁴

Similarly, the lack of significant correlations between structural and functional connectivity in this study might seem surprising. However, the associations between structural and functional connectivity may not be entirely bidirectional. For example, reductions in structural connectivity would be expected to lead to reductions in functional connectivity, but reduced functional connectivity might not diminish structural connectivity. Consequently, the absence of significant correlations between structural and functional measures is not particularly surprising because we did not see abnormalities in structural connectivity for these regions. In other words, variation in functional connectivity for these regions appears to be attributable to variation in factors other than macrostructural connectivity.

The present results show mid-level visual cortex functional connectivity in BD to be roughly intermediate to the SZ and HC groups: not significantly different from HC, but not significantly different from SZ either. It is possible that intermediate levels of dysconnectivity could result from heterogeneity within the BD group, but comparisons of common BD subtypes (BD I vs II,

history of psychosis vs no history of psychosis) revealed no significant differences. Thus, it could be that people with BD, on average, tend to be phenotypically intermediate to SZ and HC in terms of visual system functional connectivity, regardless of disorder subtype. However, future studies with larger samples of BD subtypes will be required to address this issue more fully.

Although the present results are generally consistent with the hypotheses of the study and may help to inform theoretical models of perceptual dysfunction in SZ and related disorders, the study had various limitations. First, the groups were not well matched for sex in this study. Although sex did not interact with any factors of interest, more balanced numbers of each sex across groups would be preferable. Second, it is possible that more sensitive structural connectivity measures (eg, higher-dimensional DWI) might reveal subtle group differences that were not apparent in the present analyses, and additional functional connectivity data might reveal subtle differences in EVC local efficiency. Third, patients tested in this study were on clinically determined doses of medication. We looked for and did not find any significant correlations between chlorpromazine-equivalent medication dosage and each of the graph metrics of interest. Still, a purer test of connectivity differences in unmedicated SZ and BD patients would be helpful for comparison, but such samples are extremely rare and are often unrepresentative of the diseases. Fourth, by design, this study investigated only global and local efficiency. Dozens of other graph metrics exist, and it is possible that other metrics might reveal additional information about dysconnectivity in SZ or BD. The 2 metrics we examined are calculated based on shortest-path connections between nodes, while information transfer within the brain does not necessarily follow shortest paths.⁵⁵ However, we focused only on the 2 most common metrics of local and global efficiency to minimize the likelihood of spurious findings that could result from performing many analyses not driven by strong hypotheses, and to maximize the comparability of this study to other studies in psychopathology.

A more general limitation is that the current dataset is not able to identify the specific causes of observed group differences in functional connectivity. It is possible that differences in brain structure could contribute (eg, cortical thickness differences, or differences in microstructural connectivity that are not detectable with DWI). It is also possible that functional connectivity differences are driven largely by differences in dynamic physiological processes (eg, cognitive activity during the scan). The root causes of group differences in functional connectivity and the relationships between structural and functional connectivity are important topics for future research, but the present data do not directly address these questions except insofar as correlational measures suggest that structural and functional connectivity are not highly related for the particular visual regions examined.

Despite these limitations, our study provides important, novel evidence of visual system functional dysconnectivity in SZ, and it suggests an intermediate phenotype for visual processing in BD. This evidence serves to corroborate and advance theoretical models of dysfunctional visual perception in SZ, which may provide a framework for understanding dysfunction in other cognitive domains in the future. The results also suggest that theoretical models developed to explain perceptual deficits in SZ may help to explain similar deficits in BD and other related disorders on the psychosis spectrum.

While deficits in visual perception represent only one of many cognitive domains affected in psychosis spectrum disorders, there are several reasons to believe that understanding neural factors that contribute to deficits in visual perception could be particularly fruitful for advancing understanding of fundamental features of psychosis. First, visual processing deficits appear to have important downstream effects on processing in other cognitive domains in SZ. Specifically, deficits in visual processing are associated with cascading impairments in integrative cognitive domains such as social cognition, which in turn lead to deficits in functional outcomes.⁷ Second, details of the structure and function of visual processing areas are among the best understood of any brain regions thanks to decades of painstaking neuroscientific research. This makes the visual system an excellent model neural system for which it may be possible to identify specific processing abnormalities, particularly readily and precisely. Once abnormalities within this model system have been identified, it may be easier to identify corresponding abnormalities in other brain networks involved in other cognitive processing domains that have been less precisely characterized. Third, hallucinations, one of the most characteristic symptoms of psychosis, are a perceptual phenomenon, suggesting that perceptual abnormalities in disorders such as SZ and BD could be a core feature of these illnesses.

As such, while deficits in visual perception represent only a subset of the cognitive deficits that occur in the disorder, understanding perceptual deficits may prove important for understanding psychosis more broadly. Thus, the present results, and the extension of the model of visual processing deficits in SZ that they support, provide a basis for critical future research using similar methods, with the goal of understanding processing abnormalities that contribute to poor functional outcomes in disorders of psychosis.

Supplementary Material

Supplementary data are available at *Schizophrenia Bulletin* Open online.

Funding

This project was supported by the National Institutes of Health (NIH) R01MH095878, to MFG, “Visual Tuning and Performance in Schizophrenia and Bipolar

Disorder.” EAR was also supported by the NIH under Ruth L. Kirschstein National Research Service Award F32MH108317. NIMH had no role in the design and conduct of the study; collection, management, analysis, and interpretation of the data; preparation, review, or approval of the manuscript; or decision to submit the manuscript for publication. This work used computational and storage services associated with the Hoffman2 Shared Cluster provided by UCLA Institute for Digital Research and Education’s Research Technology Group.

Acknowledgments

The authors thank Stephanie Njau and Antoni Kubicki for their assistance in DWI data processing, including visual inspection of the data for quality assurance, as well as Ana Ceci Meyers, Julio Iglesias, and other members of the Green Laboratory for their assistance in data collection. E.A.R. was previously an employee of Data Cubed LLC, a digital phenotyping company. K.H.N. has received research support for other studies from Posit Science, Inc., and Janssen and has been a consultant to Astellas, Biogen, Genentech, Janssen, MedinCell, Otsuka, Takeda, and Teva. M.F.G. has been a paid consultant for AiCure, Biogen, Lundbeck, and Roche, a member of the Scientific Board of Cadent, and has received research funds from Forum. All other authors reported no conflicts of interest.

References

- Green MF. What are the functional consequences of neurocognitive deficits in schizophrenia? *AJP*. 1996;153(3):321–330.
- Green MF, Horan WP, Lee J. Nonsocial and social cognition in schizophrenia: current evidence and future directions. *World Psychiatry*. 2019;18(2):146–161.
- Robinson LJ, Thompson JM, Gallagher P, et al. A meta-analysis of cognitive deficits in euthymic patients with bipolar disorder. *J Affect Disord*. 2006;93(1-3):105–115.
- Bortolato B, Miskowiak KW, Köhler CA, Vieta E, Carvalho AF. Cognitive dysfunction in bipolar disorder and schizophrenia: a systematic review of meta-analyses. *Neuropsychiatr Dis Treat*. 2015;11:3111–3125.
- Lynham AJ, Hubbard L, Tansey KE, et al. Examining cognition across the bipolar/schizophrenia diagnostic spectrum. *J Psychiatry Neurosci*. 2018;43(3):170076.
- Butler PD, Silverstein SM, Dakin SC. Visual perception and its impairment in schizophrenia. *Biol Psychiatry*. 2008;64(1):40–47.
- Green MF, Hellemann G, Horan WP, Lee J, Wynn JK. From perception to functional outcome in schizophrenia. *Arch Gen Psychiatry*. 2012;69(12):1216–1219.
- Javitt DC, Freedman R. Sensory processing dysfunction in the personal experience and neuronal machinery of schizophrenia. *Am J Psychiatry*. 2015;172(1):17–31.
- Javitt DC. When doors of perception close: bottom-up models of disrupted cognition in schizophrenia. *Annu Rev Clin Psychol*. 2009;5:249–275.
- Green MF, Butler PD, Chen Y, et al. Perception measurement in clinical trials of schizophrenia: promising paradigms from CNTRICS. *Schizophr Bull*. 2009;35(1):163–181.
- Jahshan C, Wynn JK, McCleery A, Glahn DC, Altshuler LL, Green MF. Cross-diagnostic comparison of visual processing in bipolar disorder and schizophrenia. *J Psychiatr Res*. 2014;51:42–48.
- Yang E, Tadin D, Glasser DM, Wook Hong S, Blake R, Park S. Visual context processing in bipolar disorder: a comparison with schizophrenia. *Front Psychol*. 2013;4:569.
- Green MF, Lee J, Cohen MS, et al. Functional neuroanatomy of visual masking deficits in schizophrenia. *Arch Gen Psychiatry*. 2009;66(12):1295–1303.
- Silverstein SM, Harms MP, Carter CS, et al. Cortical contributions to impaired contour integration in schizophrenia. *Neuropsychologia*. 2015;75:469–480.
- Lee J, Reavis EA, Engel SA, et al. fMRI evidence of aberrant neural adaptation for objects in schizophrenia and bipolar disorder. *Hum Brain Mapp*. 2019;40(5):1608–1617.
- Yoon JH, Maddock RJ, Rokem A, et al. GABA concentration is reduced in visual cortex in schizophrenia and correlates with orientation-specific surround suppression. *J Neurosci*. 2010;30(10):3777–3781.
- Wynn JK, Green MF, Engel S, et al. Increased extent of object-selective cortex in schizophrenia. *Psychiatry Res*. 2008;164(2):97–105.
- Green MF, Lee J, Wynn JK, Mathis KI. Visual masking in schizophrenia: overview and theoretical implications. *Schizophr Bull*. 2011;37(4):700–708.
- Wheeler AL, Voineskos AN. A review of structural neuroimaging in schizophrenia: from connectivity to connectomics. *Front Hum Neurosci*. 2014;8:653.
- Fornito A, Bullmore ET. Reconciling abnormalities of brain network structure and function in schizophrenia. *Curr Opin Neurobiol*. 2015;30:44–50.
- Karlsgodt KH. Diffusion imaging of white matter in schizophrenia: progress and future directions. *Biological Psychiatry: Cognitive Neuroscience and Neuroimaging*. 2016;1(3):209–217.
- Power JD, Cohen AL, Nelson SM, et al. Functional network organization of the human brain. *Neuron*. 2011;72(4):665–678.
- Rubinov M, Sporns O. Complex network measures of brain connectivity: uses and interpretations. *Neuroimage*. 2010;52(3):1059–1069.
- Achard S, Bullmore E. Efficiency and cost of economical brain functional networks. *PLoS Comput Biol*. 2007;3(2):e17.
- Bohlsen MM, Brouwer RM, Mandl RC, et al. Structural brain connectivity as a genetic marker for schizophrenia. *JAMA Psychiatry*. 2016;73(1):11–19.
- Sheffield JM, Kandala S, Tamminga CA, et al. Transdiagnostic associations between functional brain network integrity and cognition. *JAMA Psychiatry*. 2017;74(6):605–613.
- Wang Y, Deng F, Jia Y, et al. Disrupted rich club organization and structural brain connectome in unmedicated bipolar disorder. *Psychol Med*. 2019;49(3):510–518.
- Latora V, Marchiori M. Efficient behavior of small-world networks. *Phys Rev Lett*. 2001;87(19):198701.
- Jimenez AM, Riedel P, Lee J, Reavis EA, Green MF. Linking resting-state networks and social cognition in schizophrenia and bipolar disorder. *Hum Brain Mapp*. 2019;40(16):4703–4715.
- Reavis EA, Lee J, Wynn JK, et al. Linking optic radiation volume to visual perception in schizophrenia and

- bipolar disorder. *Schizophr Res*. 2017. doi:[10.1016/j.schres.2017.03.027](https://doi.org/10.1016/j.schres.2017.03.027).
31. First M, Spitzer R, Gibbon M, Williams J. *Structured Clinical Interview for DSM-IV Axis I Disorders—Patient Edition*. New York, NY: Biometrics Research Department, New York State Psychiatric Institute; 1997.
 32. Dale AM, Fischl B, Sereno MI. Cortical surface-based analysis. I. Segmentation and surface reconstruction. *Neuroimage*. 1999;9(2):179–194.
 33. Jenkinson M, Beckmann CF, Behrens TE, Woolrich MW, Smith SM. FSL. *Neuroimage*. 2012;62(2):782–790.
 34. Smith SM, Jenkinson M, Woolrich MW, et al. Advances in functional and structural MR image analysis and implementation as FSL. *NeuroImage*. 2004;23(Suppl 1):S208–S219.
 35. Tournier JD, Calamante F, Connelly A. MRtrix: diffusion tractography in crossing fiber regions. Lee J, ed. *Int J Imaging Syst Technol*. 2012;22(1):53–66.
 36. Desikan RS, Ségonne F, Fischl B, et al. An automated labeling system for subdividing the human cerebral cortex on MRI scans into gyral based regions of interest. *Neuroimage*. 2006;31(3):968–980.
 37. Glasser MF, Coalson TS, Robinson EC, et al. A multimodal parcellation of human cerebral cortex. *Nature*. 2016;536(7615):171–178.
 38. Jenkinson M, Bannister P, Brady M, Smith S. Improved optimization for the robust and accurate linear registration and motion correction of brain images. *Neuroimage*. 2002;17(2):825–841.
 39. Pruim RHR, Mennes M, van Rooij D, Llera A, Buitelaar JK, Beckmann CF. ICA-AROMA: a robust ICA-based strategy for removing motion artifacts from fMRI data. *Neuroimage*. 2015;112:267–277.
 40. Smith RE, Tournier JD, Calamante F, Connelly A. SIFT: Spherical-deconvolution informed filtering of tractograms. *Neuroimage*. 2013;67:298–312.
 41. Smith RE, Tournier JD, Calamante F, Connelly A. SIFT2: Enabling dense quantitative assessment of brain white matter connectivity using streamlines tractography. *Neuroimage*. 2015;119:338–351.
 42. Smith RE, Tournier JD, Calamante F, Connelly A. Anatomically-constrained tractography: improved diffusion MRI streamlines tractography through effective use of anatomical information. *Neuroimage*. 2012;62(3):1924–1938.
 43. Bassett DS, Nelson BG, Mueller BA, Camchong J, Lim KO. Altered resting state complexity in schizophrenia. *Neuroimage*. 2012;59(3):2196–2207.
 44. van den Heuvel MP, de Lange SC, Zalesky A, Seguin C, Yeo BTT, Schmidt R. Proportional thresholding in resting-state fMRI functional connectivity networks and consequences for patient-control connectome studies: issues and recommendations. *Neuroimage*. 2017;152:437–449.
 45. Hallquist MN, Hillary FG. Graph theory approaches to functional network organization in brain disorders: a critique for a brave new small-world. *Netw Neurosci*. 2019;3(1):1–26.
 46. Leucht S, Samara M, Heres S, Patel MX, Woods SW, Davis JM. Dose equivalents for second-generation antipsychotics: the minimum effective dose method. *Schizophr Bull*. 2014;40(2):314–326.
 47. Andreasen NC, Pressler M, Nopoulos P, Miller D, Ho BC. Antipsychotic dose equivalents and dose-years: a standardized method for comparing exposure to different drugs. *Biol Psychiatry*. 2010;67(3):255–262.
 48. Gong G, Rosa-Neto P, Carbonell F, Chen ZJ, He Y, Evans AC. Age- and gender-related differences in the cortical anatomical network. *J Neurosci*. 2009;29(50):15684–15693.
 49. Jahanshad N, Thompson PM. Multimodal neuroimaging of male and female brain structure in health and disease across the life span. *J Neurosci Res*. 2017;95(1-2):371–379.
 50. Bordier C, Nicolini C, Forcellini G, Bifone A. Disrupted modular organization of primary sensory brain areas in schizophrenia. *Neuroimage Clin*. 2018;18:682–693.
 51. Deng Y, Liu K, Cheng D, et al. Ventral and dorsal visual pathways exhibit abnormalities of static and dynamic connectivities, respectively, in patients with schizophrenia. *Schizophr Res*. 2019;206:103–110.
 52. van de Ven V, Jagiela AR, Oertel-Knöchel V, Linden DEJ. Reduced intrinsic visual cortical connectivity is associated with impaired perceptual closure in schizophrenia. *NeuroImage: Clinical*. 2017;15:45–52.
 53. Subramaniam K, Gill J, Fisher M, Mukherjee P, Nagarajan S, Vinogradov S. White matter microstructure predicts cognitive training-induced improvements in attention and executive functioning in schizophrenia. *Schizophr Res*. 2018;193(C):276–283.
 54. Reavis EA, Lee J, Wynn JK, Engel SA, Jimenez AM, Green MF. Cortical thickness of functionally defined visual areas in schizophrenia and bipolar disorder. *Cereb Cortex*. 2017;27(5):2984–2993.
 55. Avena-Koenigsberger A, Misić B, Sporns O. Communication dynamics in complex brain networks. *Nat Rev Neurosci*. 2018;19(1):17–33.